Ocean and Coastal Management 198 (2020) 105387

Contents lists available at ScienceDirect

Ocean and Coastal Management

journal homepage: http://www.elsevier.com/locate/ocecoaman

Coastal cliff exposure and management

Rafael J. Bergillos [a], Cristobal Rodriguez-Delgado [b,c], Luis Medina [d], Gregorio Iglesias [e,b,*]

[a] Hydraulic Engineering Area, Department of Agronomy, University of Cordoba, Rabanales Campus, Leonardo da Vinci Building, 14071, Córdoba, Spain
[b] School of Engineering, University of Plymouth, Plymouth, PL4 8AA, UK
[c] PROES Consultores, Calle San Germán 39, 28020, Madrid, Spain
[d] Department of Geotechnical Engineering, School of Civil Engineering, University of A Coruña, Elviña Campus, 15071, A Coruña, Spain
[e] MaREI, Environmental Research Institute & School of Engineering, University College Cork, College Road, Cork, Ireland

ARTICLE INFO

Keywords:
Cliff
Erosion
Wave
Exposure
Mapping
Management

ABSTRACT

Coastal cliffs cover about 75% of the world's coastlines. Many of these cliffs suffer severe erosion problems, which are mainly caused by wave action and lead to important damages. The main objective of this work is to propose and apply a methodology to characterize and map wave exposure levels for the management of cliff coasts. The methodology proposed consists of a number of steps. First, a statistical characterization of the wave climate in deep water is performed. Second, relevant sea states are propagated towards the cliff by means of a numerical model. Then, the results are used to assess the distribution of significant wave heights and wave power along the cliff toe. Finally, four exposure levels are defined based on the wave power values at the cliff, and exposure zones are mapped accordingly along the cliff. This approach is illustrated with a case study – the Catedrales Cliffs and Beach, a tourism hotspot in Galicia (NW Spain) where erosion caused loss of human life. We find that exposure levels are primarily influenced by the nearshore bed morphology, which controls wave refraction, shoaling and breaking, as well as by the geometry and orientation of the cliff, with some parts more exposed than others to the prevailing wave direction. On the islets off the cliff the windward faces have a greater level of exposure, since the leeward faces are protected by the islets themselves and lower water depths. The rocky outcrops that occur at the cliff toe in some sections act as emerged (submerged) breakwaters under low (high) tide conditions, dissipating wave power and thus reducing wave exposure. The methodology proposed in this work enables coastal managers to prevent the personal and material damages derived from cliff erosion by focusing remedial measures where they are most needed.

1. Introduction

Cliff coasts are the most common coastal environment across the globe (Emery and Kuhn, 1982; Bird, 2011). Some of these cliffs constitute environmental monuments. The management of these coastal environments, thus, is important for biodiversity protection (Cao et al., 2010) and for their socioeconomic value as tourism destinations. The study area in this work is a case in point: the Catedrales (Cathedrals) Cliff and Beach, a tourism hotspot in NW Spain (Fig. 1).

The case study is not unique, so that the methods and results of this paper can be extended to help manage other coastal cliffs of environmental and tourist value, such as the Azure Window (Malta), the Arco de Cabo San Lucas (Mexico), the Ponte da Piedade (Portugal), the Minamijima Island (Japan), the Durdle Door (England), the Perce Rock (Canada), the Arch Rock (Ireland), the Cuevas del Mar beach (Spain), the Portada (Chile), the Darwin Arch (Ecuador), the Porte d'Aval (France), the Moher Cliffs (Republic of Ireland), the Quebrada coast (Spain), the Twelve Apostles (Australia), the Pigeon Rocks (Lebanon), the Green Bridge (Wales), the Old Harry Rocks (England), the Sunset Cliffs (United States), the Yesnaby (Scotland), the Catedral (Peru), the Flamborough Head (England), the Thirle Door and the Stacks of Duncansby (Scotland), the Drangarnir (Faroe Islands), the Holei Sea Arch (Hawai) and the Hvitserkur (Iceland). Some of these cliffs are shown in Fig. 2.

Coastal cliffs are subject to erosion induced by wave action. Research efforts have been carried out over the last decades to characterize and model the behaviour of these coastal systems (Nunes et al., 2009; Stanchev et al., 2018; Guitián et al., 2020). In the late 70s, Sunamura (1977) proposed a relationship between cliff erosion and wave force based on laboratory and field data. More than ten years later, in the 90s,

* Corresponding author. School of Engineering, University of Plymouth, Plymouth, PL4 8AA, UK.
E-mail address: gregorio.iglesias@ucc.ie (G. Iglesias).

https://doi.org/10.1016/j.ocecoaman.2020.105387
Received 6 May 2020; Received in revised form 8 September 2020; Accepted 11 September 2020
Available online 29 September 2020

Fig. 1. Case study: Catedrales Cliffs and Beach (Galicia, NW Spain). Source: Eduardo Blanco (left photograph), Fran Nieto (right photograph).

Fig. 2. From left to right, top to bottom: Azure Window, Arco de Cabo San Lucas, Ponte da Piedade, Minamijima Island (first row); Durdle Door, Perce Rock, Arch Rock, Cuevas del Mar (second row); Portada, Porte d'Aval, Moher Cliffs, Quebrada coast (third row); Twelve Apostles, Pigeon Rocks, Green Bridge, Yesnaby (fourth row); Flamborough Head, Thirle Door, Holei Sea Arch, Hvitserkur (fifth row). Source: Google. (For interpretation of the references to colour in this figure legend, the reader is referred to the Web version of this article.)

Jones and Williams (1991) studied the factors that drive cliff erosion through measurements of annual recession, wave refraction modelling and regression analysis on the Welsh coast. In that decade, Komar and Shih (1993) and Shih and Komar (1994) also investigated the cliff erosion along the Oregon coast (US) based on tectonic controls, and on field measurements of sediment size and beach morphology, respectively.

In the 2000s, the collapse of a cliff in France was investigated by Duperret et al. (2002) through in situ examination and measurements of the deposit along with stratigraphical dating. Cliff processes on the coast of North Yoskshire, in the UK, were monitored by means of terrestrial laser scanning (Rosser et al., 2005). The role of sediments released from cliff erosion to protect low-lying coasts from flooding was also investigated in the 2000s (Dawson et al., 2009). During the last 10 years, cliff erosion has received increasing research attention, including studies based on laser scanning measurements (Lim et al., 2011; De Rose and Basher, 2011; Johnstone et al., 2016; Earlie et al., 2018; Westoby et al., 2018; Terefenko et al., 2018, 2019; Zelaya Wziatek et al., 2019; Alessio and Keller, 2020); analysis of aerial photographs (De Rose and Basher, 2011; del Río et al., 2016), terrestrial and aerial vehicle

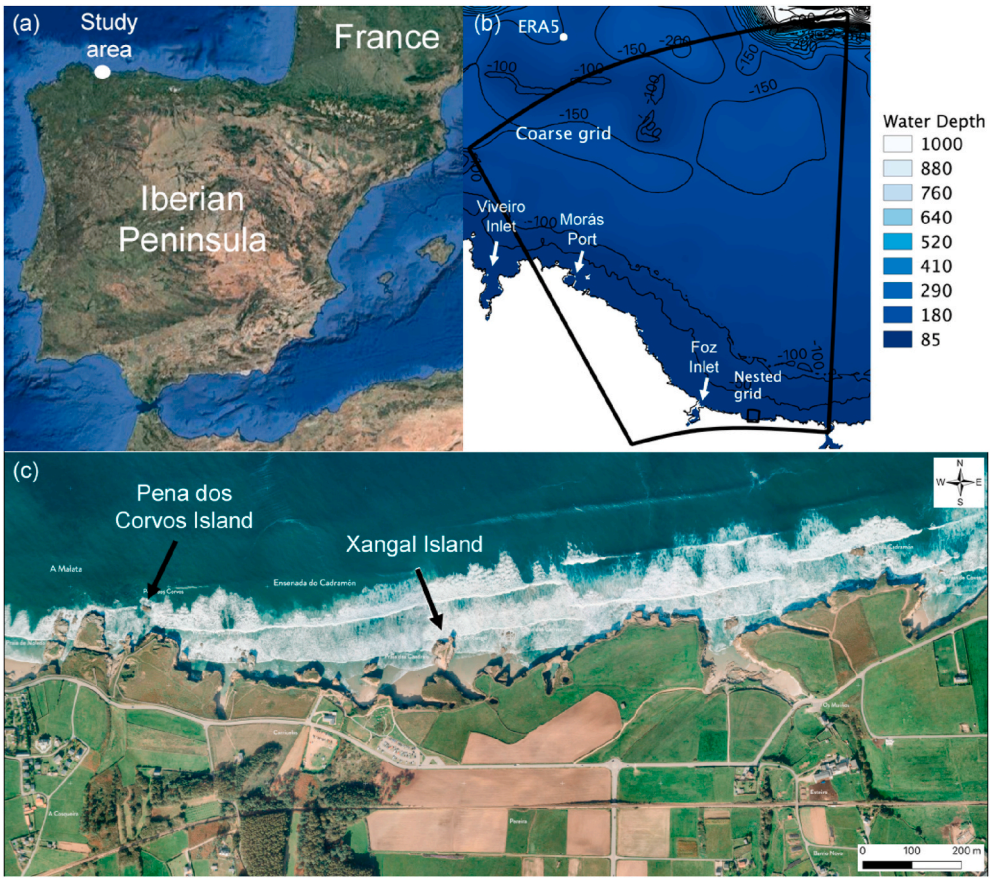

Fig. 3. (a) Location of the study area in north-western Spain (43° 33′ 14'' N, 7° 09′ 26'' W). (b) Boundaries of the computational grids used to apply the Delft3D-Wave model, distribution of water depths and location of the ERA5 point. (c) Plan view of the study area.

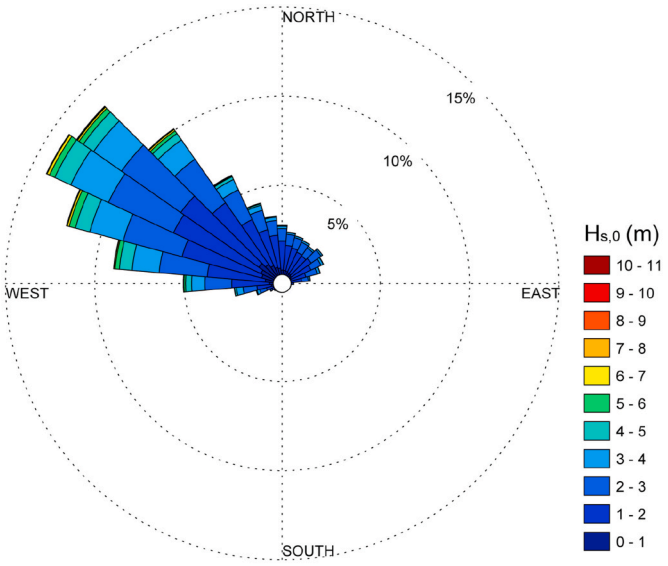

Fig. 4. Wave rose in deep water based on the ERA5 point data.

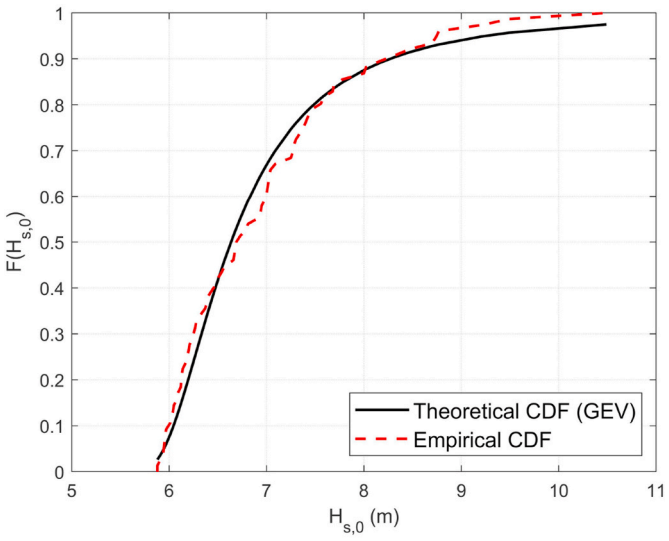

Fig. 5. Empirical and theoretical (Generalized Extreme Value, GEV) cumulative distribution functions of the deep-water significant wave height values after the application of the Peak Over Threshold (POT) method.

photogrammetry (Letortu et al., 2018), multi-view stereo (Westoby et al., 2018) and high-resolution videos (Thompson et al., 2019); and development of models and methods to predict or characterize cliff erosion (Terefenko et al., 2019; Hapke and Plant, 2010; Barlow et al., 2012; Muñoz-López et al., 2020). The information of most of the local studies addressing cliff erosion was integrated by Prémaillon et al. (2018) into the global database *GlobR2C2* (Global Recession Rates of Coastal Cliffs).

In recent years, numerous works have dealt with the modelling of extreme waves for different purposes. Some representative examples are the study of the implications of the erosion of deltas on wave

Table 1
Deep-water sea states propagated with the numerical model [T_r: return period; $H_{s,0}$: significant wave height in deep water; T_p: spectral peak period in deep water; θ: mean incoming wave direction in deep water].

T_r (years)	$H_{s,0}$ (m)	T_p (s)	θ (°)
2	6.6	15	300
10	8.3	15	300
50	11	15	300
100	12.7	15	300

propagation and longshore sediment transport (Bergillos et al., 2016a), the coupling of cross-shore and longshore sediment transport to reproduce the evolution of the beach profile (Bergillos et al., 2017a) or the analysis of the effects of wave farms on coastal areas (Bergillos et al., 2018a, 2019a, 2019b, 2019c; Rodriguez-Delgado et al., 2018a, 2018b, 2019a, 2019b, 2019c). Statistical techniques have also been used for a number of coastal management applications, such as the forecasting of the efficiency of nourishment projects (Bergillos et al., 2018b), the long-term simulation of the performance of wave energy converter arrays (López-Ruiz et al., 2018a, 2018b) or the assessment of the operational conditions of infrastructures located in coastal areas (Rodriguez-Delgado et al., 2020), among others. However, to our best knowledge neither modelling of extreme waves nor statistical analysis have been applied to quantify wave power and exposure on coastal cliffs for management purposes.

The main objective of this paper is to propose and apply a methodology to characterize and map wave exposure zones to support the management of coastal cliffs. This methodology is applied to the Catedrales cliffs in NW Spain. The manuscript is structured as follows. Section 2 presents the main characteristics of the study area. Section 3 details the extreme value analysis of the wave data in deep water, the set-up of the wave propagation model and the computation of significant wave height and wave power along the cliff toe. In Section 4, the results of the application of the methodology to the case study are reported. These results and some management applications are discussed in Section 5. Finally, the conclusions are drawn in Section 6.

2. Study area

The Catedrales cliffs are located in north-western Spain, facing the Atlantic Ocean (Fig. 3). This 1700-m-long coastal stretch was declared *Natural Monument* by the Galician Regional Government in 2005.

The prevailing wave direction in the study area is north-west (Fig. 4). This is the result of the location of the cliff in the north-west of the Iberian Peninsula, where the Atlantic swell is predominant. The wave climate in this region is particularly energetic (Carballo et al., 2015; Carballo et al., 2015b; Veigas et al., 2015), with deep-water significant wave heights exceeding 10 m under storm conditions (Fig. 4).

Cliff erosion causes material damages and poses risks to human life. A clear example of these risks was the death of a person in March 2018 due to the impact of a rock detached from a cliff in the study area. Given the high numbers of visitors and the mentioned erosion issues, the definition and mapping of wave exposure zones is necessary to facilitate the management of this tourism hotspot.

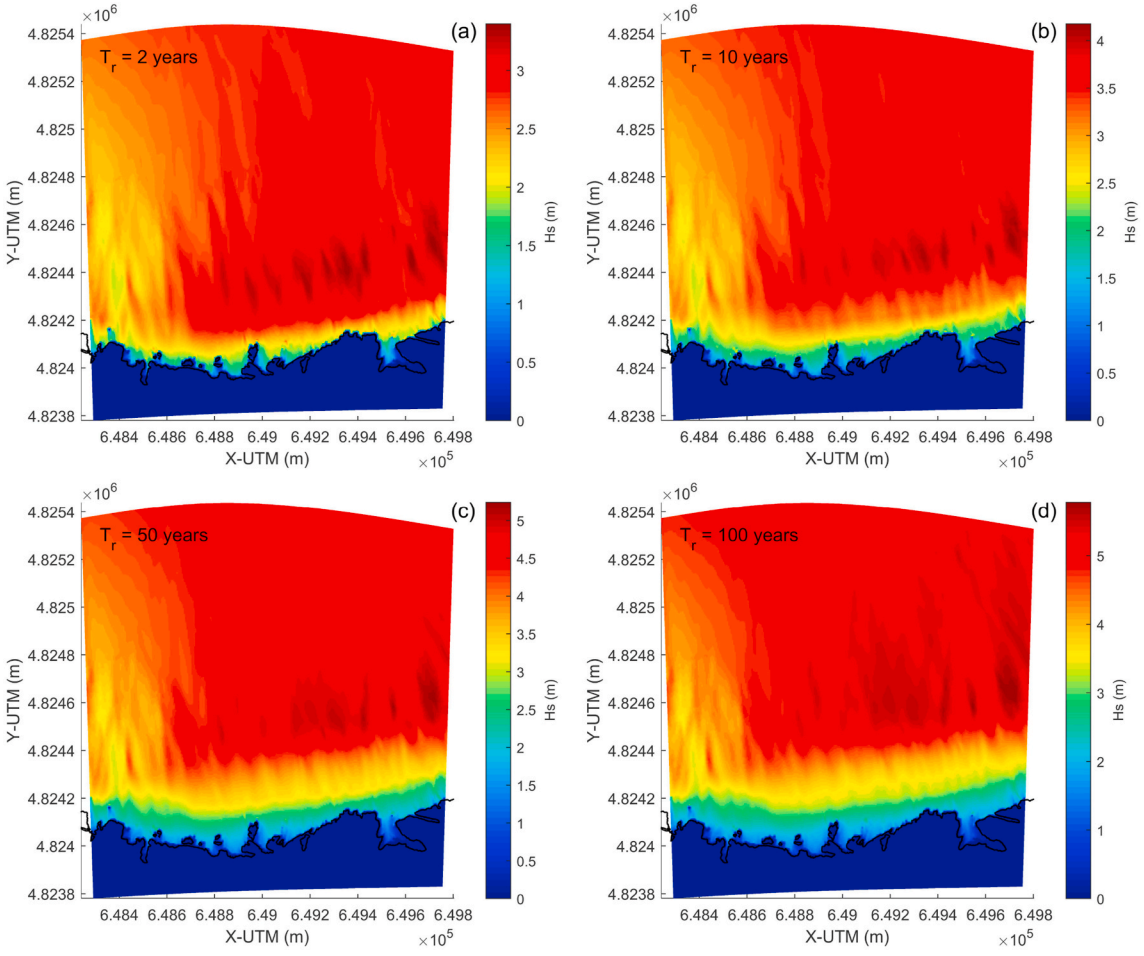

Fig. 6. Plan view distribution of the significant wave heights for four return period (T_r) values: (a) $T_r = 2$ years, (b) $T_r = 10$ years, (c) $T_r = 50$ years and (d) $T_r = 100$ years.

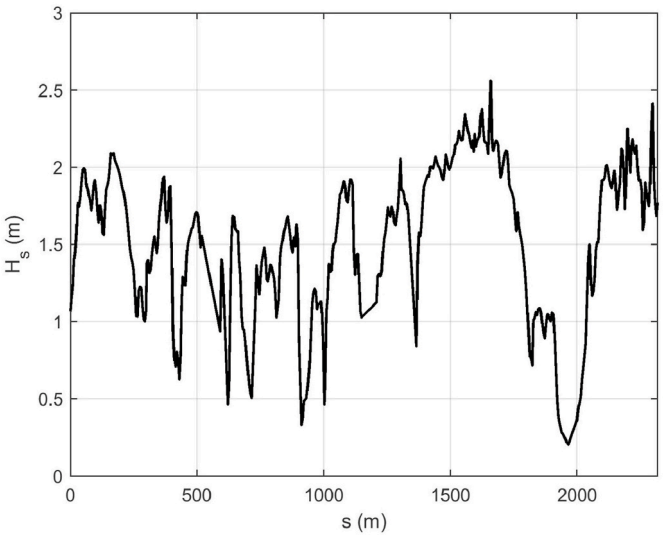

Fig. 7. Significant wave height along the cliff toe ($T_r = 2$ years).

3. Materials and methods

Although wave action is not the sole factor causing cliff erosion, it is one of the most important. Thus, it is essential to analyse the extreme wave variables in deep water as well as the modification of the wave parameters as the wave propagates from deep water towards the coast. To this end, we first perform a statistical analysis of the wave climate in deep water off the cliff. Then, representative sea states are numerically propagated toward the nearshore region to determine the distribution of wave power along the cliff toe. This section firstly describes the analysis of deep-water extreme values of significant wave heights, since cliff erosion is mainly generated by these extreme values. Later, we describe how the sea states in deep water are propagated toward the cliff through a numerical model. Finally, the procedure to calculate wave height and power along the cliff toe is presented.

3.1. Extreme value analysis of the offshore wave climate

The analysis of extreme wave values was based on the ERA5 model data of the European Centre for Medium-Range Weather Forecast (ECMWF). This is a global model, with a grid resolution of 0.5° x 0.5°. In each node of the grid, the model provides the significant wave height, the spectral peak period and the incoming mean wave direction, among others ocean and meteorological variables. For this work, the wave data of a node located at a latitude of 44° N and a longitude of 7.5° W were used.

As previously mentioned, from the point of view of cliff erosion, it is advisable to statistically analyse the extreme wave regime. For that, the Peak Over Threshold (POT) method (Goda, 2010) was applied to the significant wave height data, considering as threshold value the wave height value that is not exceeded during 99% of the time ($H_T = H_{99\%}$). Once the POT method was applied, several cumulative distribution functions (CDFs) were fitted to the extreme values obtained and the best fit was provided by the Generalized Extreme Value (GEV) function. Finally, based on the GEV function, the wave height values associated to return periods of 2, 10, 50 and 100 years were obtained.

3.2. Numerical wave propagation model

The wave height values mentioned in the previous section, along with the most frequent values of spectral peak period and mean wave direction under storm conditions, were propagated from the ERA5 node location towards the cliff by means of the WAVE module of the Delft3D model, which is based on the SWAN (Simulating WAves Nearshore) model (Holthuijsen et al., 1993; Booij et al., 1999). The wave propagations were carried out under high tide conditions. The Delft3D-WAVE model reproduces the main wave propagation processes, such as refraction, shoaling, breaking, reflection and diffraction induced by obstacles, bottom friction, non-linear wave-interactions, and white-capping. This model has been widely applied in ocean and coastal engineering (Bergillos et al., 2016a, 2016b, 2017a, 2017b, 2018a, 2018b, 2019a, 2019b, 2019c; Rodriguez-Delgado et al., 2018a, 2018b, 2019a, 2019b, 2019c, 2020; Abanades et al., 2018; Astariz et al., 2018; Kompor et al., 2018; Magaña et al., 2018; Poppema et al., 2019; Reyes-Merlo et al., 2017; Stronkhorst et al., 2018; Różyński et al., 2019; Van Der Werf et al., 2019; Waldman et al., 2017).

Apart from wave and tide, topographic and bathymetric data are required as input by the model. These data were measured during a field survey conducted by *Nucleo Galicia S.L.* in the framework of this study. The multibeam bathymetric measurements were conducted along 38 shore-normal profiles, covering a surface of 1700 m (alongshore) x 2000 m (cross-shore). Along each profile measurements were collected every 4 m. The bathymetric data were complemented with topographic measurements that covered not only the emerged area of the study site, but

Table 2
Wave exposure levels [*P*, wave power acting on the cliff].

Exposure type	Wave power
Low wave exposure	$P \leq 4.6\text{kWm}^{-1}$
Middle wave exposure	$4.6\text{kWm}^{-1} < P \leq 9.2\text{kWm}^{-1}$
High wave exposure	$9.2\text{kWm}^{-1} < P \leq 13.8\text{kWm}^{-1}$
Extreme wave exposure	$P > 13.8\text{kWm}^{-1}$

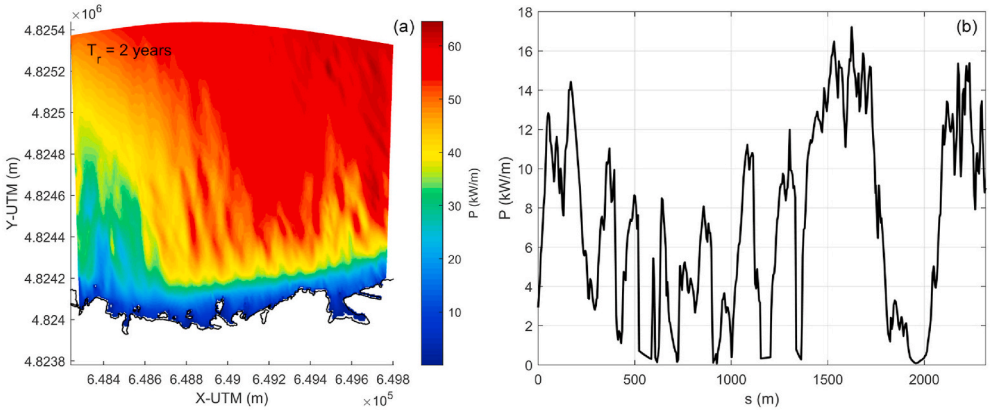

Fig. 8. (a) Plan view distribution of the wave power for a return period $T_r = 2$ years. (b) Alongshore distribution of the wave power at the cliff toe ($T_r = 2$ years).

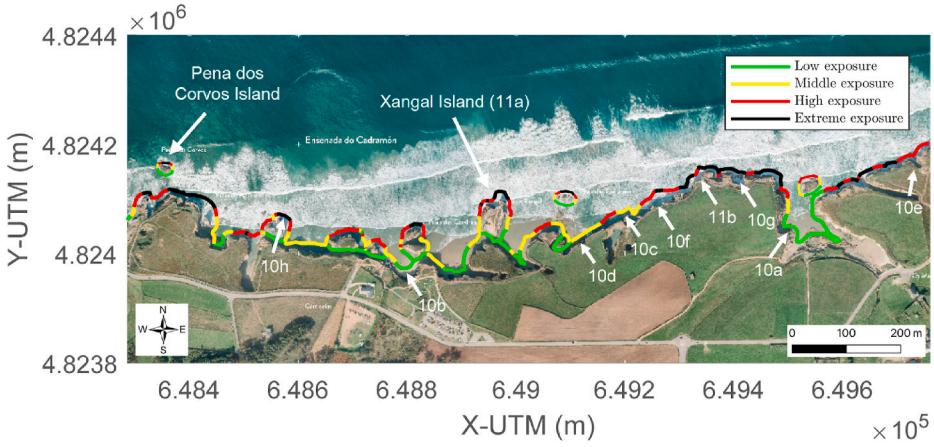

Fig. 9. Mapping of wave exposure levels onto the study area. The locations of the images of Figs. 10 and 11 are indicated.

also the shallower submerged area (up to the 1 m contour). The errors of the instruments used for the bathymetric and topographic measurements are lower than 2 cm. The measurements of bathymetry collected were complemented in deep water (up to a water depth of 1000 m) with the EMODnet (European Marine Observation and Data network) bathymetric data (Thierry et al., 2019).

The computational domain defined to perform the wave propagation consisted of two grids: (1) a coarse grid covering a wide region from the ERA5 model node to the coastline, with grid sizes from 300 m × 300 m–100 m × 100 m, and (2) a nested grid covering the nearshore region, with grid sizes from 50 m × 50 m–10 m × 10 m (Fig. 3b).

3.3. Assessment of wave height and wave power along the cliff toe

The results of the wave propagation model were used to obtain the distribution of significant wave heights along the cliff. They were also employed to compute the wave power values at the cliff toe, which can be obtained from the spectral output of the wave propagation model through the equation:

$$P = \rho g \int_0^{2\pi} \int_0^{\infty} S(f,\theta) c_g(f,h) df d\theta \quad (1)$$

where ρ is the density of salt water, g is the acceleration due to gravity, $S(f,\theta)$ is the directional wave spectrum, f is the frequency, θ is the direction of propagation of the spectral component, C_g is the group celerity and h is the water depth. Considering the integrated parameters evaluated from the spectrum, Eq. (1) can be approximated by (Besio et al., 2016):

$$P = \frac{1}{16} \rho g H_{m0}^2 C_g \ , \quad (2)$$

where H_{m0} is the spectral wave height evaluated from the wave energy spectrum and C_g is obtained as (Contestabile et al., 2015):

$$C_g = \frac{c}{2}\left(1 + \frac{2kh}{\sinh(2kh)}\right)\sqrt{\frac{g}{h}\tanh(kh)} \ , \quad (3)$$

where c is the wave celerity, k is the wave number and h is the water depth.

4. Results

4.1. Wave propagation patterns for different return periods

The fit of the GEV cumulative distribution function to the empirical CDF is shown in Fig. 5. Based on this fitted GEV function, the wave height values associated to return periods of 2, 10, 50 and 100 years were obtained. These wave height values, along with the most typical peak period and mean direction values under high-energy conditions, are shown in Table 1. These sea states were propagated toward the cliff toe for high-tide conditions by means of the wave propagation model presented in Section 3.2.

The maximum values of significant wave heights within the nested grid (Fig. 6), obtained from the wave propagation model, range from 3.3 m for a return period of 2 years–5.5 m for a return period of 100 years. As can be observed in Fig. 6, these differences in wave heights occur at deep and intermediate depths, but not at the cliff toe, since as waves approach the cliff toe, the wave heights are reduced mainly due to depth-induced wave breaking. Thus, the significant wave heights at the cliff toe do not vary between the different return periods, as they are dependent on (i.e., limited by) the water depth.

It is also observed that, in the western part of the coast, the wave heights are lower along a shore-normal section (represented in yellow in Fig. 6). This is caused by the lower depths in this area, which induce wave breaking farther away from the shoreline. The rest of variations in significant wave heights are mainly due to refraction and shoaling during the propagation of waves over a complex and irregular morphology.

4.2. Wave height and power distribution along the cliff toe

As described in the previous section, the wave heights at the toe of the cliff do not vary with the return period, as these wave heights are limited by the water depth. For this reason, in order to assess the wave impact over the cliff, the significant wave heights along the cliff toe were extracted from the results for a 2-year return period, i.e., for a deep-water significant wave height equal to 6.6 m. The results are shown in Fig. 7.

It is apparent that the significant wave heights vary significantly along the cliff toe. This is due to the effects of wave refraction and shoaling over a complex and irregular bathymetry, as well as to the geometry and orientation of the cliff, with some parts more exposed to the wave action than others.

Based on the results of the wave propagation model, both the plan view distribution and the alongshore variation along the cliff toe of wave power were assessed (Fig. 8). As in the case of significant wave heights, it is clearly observed how the depth-induced wave breaking reduces the wave power impinging. In addition, the lower water depths at the western part of the cliff, which lead to lower significant wave height values in this zone (Fig. 6), also reduce the wave power values (Fig. 8a).

The wave power distribution along the cliff toe is also highly irregular (Fig. 8b). This is induced by the aforementioned complex bathymetry and different orientations of the cliff, which induce varying

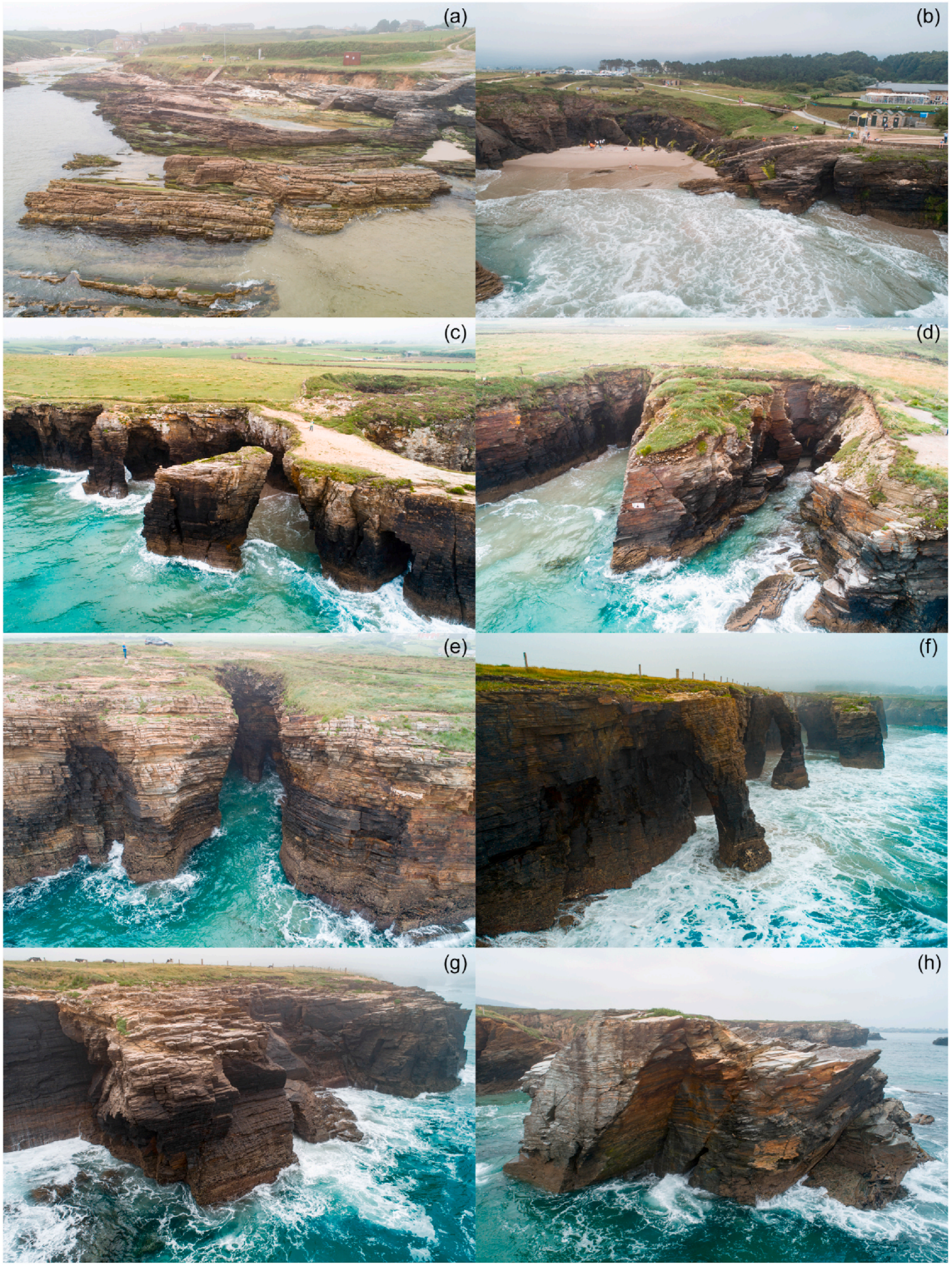

Fig. 10. Different exposure zones in the study area. From top to bottom: low exposure (a–b), middle exposure (c–d), high exposure (e–f) and extreme exposure (g–h). The locations of the images are indicated in Fig. 9.

significant wave heights at the toe (Fig. 7) and, consequently, a variable wave power distribution along the toe (Fig. 8b). This wave power distribution at the cliff toe results in different levels of exposure along the cliff, as explained in the following section.

4.3. *Wave exposure levels*

Based on the wave power values at the cliff toe, four wave exposure levels with equal ranges between 0 and the maximum wave power value at the cliff toe ($P = 13.8$ kWm^{-1}) were defined, as indicated in Table 2. The wave exposure levels were mapped onto the study area, resulting in different wave exposure zones (Figs. 9 and 10).

Fig. 11. (a) Xangal Islet. (b) Rocky outcrops at the cliff toe. The locations of the images are indicated in Fig. 9.

The wave exposure levels are primarily influenced by the orientation and geometry of the cliff, as well as by the nearshore seabed morphology (bathymetry), which controls wave refraction, shoaling and breaking. These processes determine the significant wave height that reaches the cliff toe and, therefore, the distribution of wave power along the cliff.

It may be observed that the inlet in the eastern part of the study area is classified as *low exposure* (Fig. 9) due to the lower wave power values at the inlet location (Fig. 8b, $s \approx 2000$ m). The Xangal Islet, which is located in the central part of the study area (Figs. 9–11a), has levels of exposure high and extreme on its windward face and a low level of exposure on its leeward face due to the protection provided by the islet itself and the lower water depths. On the west side of the islet, the exposure is greater than on the east side due to the prevailing wave direction (Fig. 4 and Table 1).

The Pena dos Corvos Islet, which is located in the western part (Figs. 3c and 9), induces a wave exposure variation similar to that reported in the previous paragraph for the Xangal Islet, with a greater level of exposure on the windward face of the islet (high and extreme exposures) and a lower level on the leeward face (low exposure). In the stretches where there are rocky outcrops at the toe of the cliff (Fig. 11b), the level of exposure is also reduced, but the reduction is lower than in the cases of the Xangal and Pena dos Corvos islets, since the protection provided by the islets is greater than that provided by the rocky outcrops (Fig. 11). Under high (low) tide conditions, these outcrops (Fig. 11b) act as submerged (emerged) detached breakwaters, mitigating the wave power that reaches the cliff toe.

5. Discussion

Numerous works have focused on the characterization and modelling of cliff coasts, with an approach different from the present research. For this reason, despite the valuable results and research advances reported in previous works (see Introduction), it is not easy to establish direct comparisons with the present work.

In general, the wave power acting on the cliff toe was not calculated, with one exception, Zelaya Wziatek et al. (2019). In this case, however, wave power at the cliff toe was calculated using a much simpler approach (Snell's Law) which, strictly speaking, is valid only in the case of a parallel bathymetry – certainly not in the case of the Catedrales beach and cliffs. At any rate, the wave power values in the area of study of Zelaya Wziatek et al. (2019) are far smaller (between 1.179 kW/m and 2.78 kW/m) than those obtained in the present work (Table 2), indicating a milder wave climate.

Sunamura (1977) studied another cliff coast with erosion problems. In their work cliff erosion was found to be caused only by the hydraulic action of waves. The alongshore variation in wave height in front of the cliff is not dissimilar from the results in this work (Fig. 7).

So far, the numerical modelling of the propagation of extreme waves had not been combined with statistical analysis to characterize and map wave exposure on cliff coasts and, thus, support their management. This new approach can help prevent personal and material damages derived from cliff erosion by allowing coastal managers to focus preventive measures on the sections of a cliff where they are most needed.

In the case of the Catedrales cliffs and beach it follows that cliff management measures should be varied alongshore according to the wave exposure levels obtained in this work (Fig. 9). The areas of high or extreme wave exposure should be demarcated to prevent public access, which might lead to accidents and even loss of life (as was the case on the Catedrales cliffs in 2018). On the other hand, access may be allowed to zones of middle or low wave exposure (Fig. 9). In these zones, wooden walkways with handrails could be erected along the cliff top and connected with pathways to the beach. The walkways should be slightly raised above the ground to allow the flow of runoff and avoid adverse effects on the coastal flora.

This cliff management strategy, based on measures which vary alongshore, i.e., between different sections of the cliff, is in line with the recommendation by Komar and Shih (1993) that set-back distances along the Oregon coastal cliffs – yet another area with erosion problems – be varied alongshore.

6. Conclusions

In this work, a methodology was proposed to characterize and map wave exposure levels for the management of cliff coasts. The methodology was illustrated with a case study in north-western Spain – the Catedrales Cliffs and Beach, a tourism hotspot where erosion led to loss of human life in the recent past (2018).

It was found that there are no differences in the significant wave heights acting on the cliff between the different return periods considered. This is due to depth-induced wave breaking. On this basis, the sea state associated to a 2-year return period was selected to calculate the values of significant wave height and wave power at the cliff toe – both of which were found to vary significantly along the cliff. These variations are caused by the irregular bathymetry of the study area, which controls wave refraction, shoaling and breaking, as well as by the geometry and variable orientation of the cliff, with some parts more exposed than others to the predominant wave direction.

Four exposure levels were defined based on wave power at the cliff toe: low, middle, high and extreme wave exposure. These levels were then mapped onto the cliff, resulting in different exposure zones. For instance, the inlet in the eastern part of the study area is categorized as low exposure, with wave power values below 4.6 kW/m. In some sections, the rocky outcrops at the cliff toe act as emerged (submerged) maritime structures under low (high) tide conditions, dissipating wave power and thus reducing the wave exposure of the cliff face. These sections typically belong to low or middle exposure zones. As for the islets in front of the cliff, the windward faces belong to high or even extreme exposure types, with wave power values topping 9.2 kW/m. On the contrary, the leeward faces are in the low exposure type, as they are protected from incoming wave energy by the islets themselves.

The methodology presented and applied in this work, which was developed to assist coastal managers, allows connecting wave action to

cliff exposure in a quantitative manner by defining and mapping wave exposure levels. Despite the possibles uncertainties associated with the accuracy of wave data, bathymetric measurements and/or numerical predictions, the methodology is useful for the management of coastal cliffs, and could thus help prevent or mitigate the negative effects of wave-induced cliff erosion on ownerships, infrastructures or human life.

Declaration of competing interest

The authors declare that they have no known competing financial interests or personal relationships that could have appeared to influence the work reported in this paper.

Acknowledgements

This work was carried out in the framework of the project "Study to establish the current geological and geotechnical situation of the natural monument Catedrales beach and its possible evolution in time", which was funded by the *Xunta the Galicia* (Spain) and the European Union. Rafael Bergillos was funded by the Ministerio de Ciencia Innovación y Universidades of Spain (*Programa Juan de la Cierva 2017*; FJCI-2017-31781) and Cristobal Rodriguez-Delgado was partly funded by the University of Plymouth (United Kingdom). We thank four anonymous reviewers for their helpful suggestions to improve this work.

References

Abanades, J., Flor-Blanco, G., Flor, G., Iglesias, G., 2018. Dual wave farms for energy production and coastal protection. Ocean Coast Manag. 160, 18–29.
Alessio, P., Keller, E.A., 2020. Short-term patterns and processes of coastal cliff erosion in Santa Barbara, California. Geomorphology 353, 106994.
Astariz, S., Vazquez, A., Sánchez, M., Carballo, R., Iglesias, G., 2018. Co-located wave-wind farms for improved O&M efficiency. Ocean Coast Manag. 163, 66–71.
Barlow, J., Lim, M., Rosser, N., Petley, D., Brain, M., Norman, E., Geer, M., 2012. Modeling cliff erosion using negative power law scaling of rockfalls. Geomorphology 139, 416–424.
Bergillos, R.J., López-Ruiz, A., Ortega-Sánchez, M., Masselink, G., Losada, M.A., 2016a. Implications of delta retreat on wave propagation and longshore sediment transport-Guadalfeo case study (southern Spain). Mar. Geol. 382, 1–16.
Bergillos, R.J., Masselink, G., McCall, R.T., Ortega-Sánchez, M., 2016b. Modelling overwash vulnerability along mixed sand-gravel coasts with XBeach-G: case study of Playa Granada, southern Spain. Coastal Engineering Proceedings 1 (35), 13.
Bergillos, R.J., Masselink, G., Ortega-Sánchez, M., 2017a. Coupling cross-shore and longshore sediment transport to model storm response along a mixed sand-gravel coast under varying wave directions. Coast. Eng. 129, 93–104.
Bergillos, R.J., Rodríguez-Delgado, C., Ortega-Sánchez, M., 2017b. Advances in management tools for modeling artificial nourishments in mixed beaches. J. Mar. Syst. 172, 1–13.
Bergillos, R.J., Lopez-Ruiz, A., Medina-Lopez, E., Monino, A., Ortega-Sanchez, M., 2018a. The role of wave energy converter farms on coastal protection in eroding deltas, Guadalfeo, southern Spain. J. Clean. Prod. 171, 356–367.
Bergillos, R.J., López-Ruiz, A., Principal-Gómez, D., Ortega-Sánchez, M., 2018b. An integrated methodology to forecast the efficiency of nourishment strategies in eroding deltas. Sci. Total Environ. 613, 1175–1184.
Bergillos, R.J., Rodriguez-Delgado, C., Iglesias, G., 2019a. Wave farm impacts on coastal flooding under sea-level rise: a case study in southern Spain. Sci. Total Environ. 653, 1522–1531.
Bergillos, R.J., Rodriguez-Delgado, C., Allen, J., Iglesias, G., 2019b. Wave energy converter configuration in dual wave farms. Ocean. Eng. 178, 204–214.
Bergillos, R.J., Rodriguez-Delgado, C., Allen, J., Iglesias, G., 2019c. Wave energy converter geometry for coastal flooding mitigation. Sci. Total Environ. 668, 1232–1241.
Besio, G., Mentaschi, L., Mazzino, A., 2016. Wave energy resource assessment in the Mediterranean Sea on the basis of a 35-year hindcast. Energy 94, 50–63.
Bird, E.C., 2011. Coastal Geomorphology: an Introduction. John Wiley & Sons.
Booij, N., Ris, R.C., Holthuijsen, L.H., 1999. A third-generation wave model for coastal regions: 1. Model description and validation. J. Geophys. Res.: Oceans 104, 7649–7666.
Cao, S., Ye, H., Zhan, Y., 2010. Cliff roads: an ecological conservation technique for road construction in mountainous regions of China. Landsc. Urban Plann. 94, 228–233.
Carballo, R., Sánchez, M., Ramos, V., Fraguela, J., Iglesias, G., 2015. Intra-annual wave resource characterization for energy exploitation: a new decision-aid tool. Energy Convers. Manag. 93, 1–8.
Carballo, R., Sánchez, M., Ramos, V., Fraguela, J., Iglesias, G., 2015b. The intra-annual variability in the performance of wave energy converters: a comparative study in N Galicia (Spain). Energy 82, 138–146.
Contestabile, P., Ferrante, V., Vicinanza, D., 2015. Wave energy resource along the coast of Santa Catarina (Brazil). Energies 8, 14219–14243.
Dawson, R.J., Dickson, M.E., Nicholls, R.J., Hall, J.W., Walkden, M.J., Stansby, P.K., Mokrech, M., Richards, J., Zhou, J., Milligan, J., Jordan, A., Pearson, S., Rees, J., Bates, P.D., Koukoulas, S., Watkinson, A.R., 2009. Integrated analysis of risks of coastal flooding and cliff erosion under scenarios of long term change. Climatic Change 95, 249–288.
De Rose, R.C., Basher, L.R., 2011. Measurement of river bank and cliff erosion from sequential LIDAR and historical aerial photography. Geomorphology 126, 132–147.
del Río, L., Gracia, F.J., Benavente, J., 2016. Multiple-source cliff erosion in southern Spain: current risk and future perspectives. J. Coast Res. 75, 1072–1076.
Duperret, A., Genter, A., Mortimore, R.N., Delacourt, B., De Pomerai, M.R., 2002. Coastal rock cliff erosion by collapse at Puys, France: the role of impervious marl seams within chalk of NW Europe. J. Coast Res. 52–61.
Earlie, C., Masselink, G., Russell, P., 2018. The role of beach morphology on coastal cliff erosion under extreme waves. Earth Surf. Process. Landforms 43, 1213–1228.
Emery, K., Kuhn, G., 1982. Sea cliffs: their processes, profiles, and classification. Geol. Soc. Am. Bull. 93, 644–654.
Goda, Y., 2010. Random Seas and Design of Maritime Structures, 33. World Scientific Publishing Company.
Guitián, M.A.R., Real, C., Ramil-Rego, P., Franco, R.R., Castro, H.L., 2020. Characteristics, vulnerability and conservation value of active tufa-forming springs on coastal cliffs in the NW Iberian Peninsula. Ocean Coast Manag. 189, 105122.
Hapke, C., Plant, N., 2010. Predicting coastal cliff erosion using a bayesian probabilistic model. Mar. Geol. 278, 140–149.
Holthuijsen, L., Booij, N., Ris, R., 1993. A Spectral Wave Model for the Coastal Zone. ASCE.
Johnstone, E., Raymond, J., Olsen, M.J., Driscoll, N., 2016. Morphological expressions of coastal cliff erosion processes in San Diego County. J. Coast Res. 76, 174–184.
Jones, D., Williams, A., 1991. Statistical analysis of factors influencing cliff erosion along a section of the West Wales coast, UK. Earth Surf. Process. Landforms 16, 95–111.
Komar, P.D., Shih, S.-M., 1993. Cliff erosion along the Oregon coast: a tectonic-sea level imprint plus local controls by beach processes. J. Coast Res. 747–765.
Kompor, W., Ekkawatpanit, C., Kositgittiwong, D., 2018. Assessment of ocean wave energy resource potential in Thailand. Ocean Coast Manag. 160, 64–74.
Letortu, P., Jaud, M., Grandjean, P., Ammann, J., Costa, S., Maquaire, O., Davidson, R., Le Dantec, N., Delacourt, C., 2018. Examining high-resolution survey methods for monitoring cliff erosion at an operational scale. GIScience Remote Sens. 55, 457–476.
Lim, M., Rosser, N.J., Petley, D.N., Keen, M., 2011. Quantifying the controls and influence of tide and wave impacts on coastal rock cliff erosion. J. Coast Res. 27, 46–56.
López-Ruiz, A., Bergillos, R.J., Raffo-Caballero, J.M., Ortega-Sánchez, M., 2018a. Towards an optimum design of wave energy converter arrays through an integrated approach of life cycle performance and operational capacity. Appl. Energy 209, 20–32.
López-Ruiz, A., Bergillos, R.J., Lira-Loarca, A., Ortega-Sánchez, M., 2018b. A methodology for the long-term simulation and uncertainty analysis of the operational lifetime performance of wave energy converter arrays. Energy 153, 126–135.
Magaña, P., Bergillos, R.J., Del-Rosal-Salido, J., Reyes-Merlo, M.A., Díaz-Carrasco, P., Ortega-Sánchez, M., 2018. Integrating complex numerical approaches into a user-friendly application for the management of coastal environments. Sci. Total Environ. 624, 979–990.
Muñoz-López, P., Payo, A., Ellis, M.A., Criado-Aldeanueva, F., Jenkins, G.O., 2020. A method to extract measurable indicators of coastal cliff erosion from topographical cliff and beach profiles: application to north norfolk and suffolk, east england, UK. J. Mar. Sci. Eng. 8, 20.
Nunes, M., Ferreira, Ó., Schaefer, M., Clifton, J., Baily, B., Moura, D., Loureiro, C., 2009. Hazard assessment in rock cliffs at Central Algarve (Portugal): a tool for coastal management. Ocean Coast Manag. 52, 506–515.
Poppema, D.W., Willemsen, P.W., de Vries, M.B., Zhu, Z., Borsje, B.W., Hulscher, S.J., 2019. Experiment-supported modelling of salt marsh establishment. Ocean Coast Manag. 168, 238–250.
Prémaillon, M., Regard, V., Dewez, T.J., Auda, Y., 2018. GlobR2C2 (Global Recession Rates of Coastal Cliffs): a global relational database to investigate coastal rocky cliff erosion rate variations. Earth Surface Dynamics 6, 651.
Reyes-Merlo, M.Á., Ortega-Sánchez, M., Díez-Minguito, M., Losada, M.A., 2017. Efficient dredging strategy in a tidal inlet based on an energetic approach. Ocean Coast Manag. 146, 157–169.
Rodriguez-Delgado, C., Bergillos, R.J., Ortega-Sánchez, M., Iglesias, G., 2018a. Protection of gravel-dominated coasts through wave farms: layout and shoreline evolution. Sci. Total Environ. 636, 1541–1552.
Rodriguez-Delgado, C., Bergillos, R.J., Ortega-Sánchez, M., Iglesias, G., 2018b. Wave farm effects on the coast: the alongshore position. Sci. Total Environ. 640, 1176–1186.
Rodriguez-Delgado, C., Bergillos, R.J., Iglesias, G., 2019a. Dual wave energy converter farms and coastline dynamics: the role of inter-device spacing. Sci. Total Environ. 646, 1241–1252.
Rodriguez-Delgado, C., Bergillos, R.J., Iglesias, G., 2019b. Dual wave farms for energy production and coastal protection under sea level rise. J. Clean. Prod. 222, 364–372.
Rodriguez-Delgado, C., Bergillos, R.J., Iglesias, G., 2019c. An artificial neural network model of coastal erosion mitigation through wave farms. Environ. Model. Software 119, 390–399.
Rodriguez-Delgado, C., Bergillos, R.J., Iglesias, G., 2020. Coastal infrastructure operativity against flooding – a methodology. Sci. Total Environ. 719, 137452.

Rosser, N., Petley, D., Lim, M., Dunning, S., Allison, R., 2005. Terrestrial laser scanning for monitoring the process of hard rock coastal cliff erosion. Q. J. Eng. Geol. Hydrogeol. 38, 363–375.
Różyński, G., Bielecka, M., Schönhofer, J., 2019. Application of systems approach framework (SAF) to the vistula lagoon case in Poland. Ocean Coast Manag. 168, 90–102.
Shih, S.-M., Komar, P.D., 1994. Sediments, beach morphology and sea cliff erosion within an Oregon coast littoral cell. J. Coast Res. 144–157.
Stanchev, H., Stancheva, M., Young, R., Palazov, A., 2018. Analysis of shoreline changes and cliff retreat to support marine spatial planning in shabla municipality, northeast Bulgaria. Ocean Coast Manag. 156, 127–140.
Stronkhorst, J., Huisman, B., Giardino, A., Santinelli, G., Santos, F.D., 2018. Sand nourishment strategies to mitigate coastal erosion and sea level rise at the coasts of Holland (The Netherlands) and Aveiro (Portugal) in the 21st century. Ocean Coast Manag. 156, 266–276.
Sunamura, T., 1977. A relationship between wave-induced cliff erosion and erosive force of waves. J. Geol. 85, 613–618.
Terefenko, P., Giza, A., Paprotny, D., Kubicki, A., Winowski, M., 2018. Cliff retreat induced by series of storms at Miedzyzdroje (Poland). J. Coast Res. 181–185.
Terefenko, P., Paprotny, D., Giza, A., Morales-Nápoles, O., Kubicki, A., Walczakiewicz, S., 2019. Monitoring cliff erosion with LiDAR surveys and bayesian network-based data analysis. Rem. Sens. 11, 843.
Thierry, S., Dick, S., George, S., Benoit, L., Cyrille, P., 2019. EMODnet Bathymetry a compilation of bathymetric data in the European waters. In: OCEANS 2019-Marseille. IEEE, pp. 1–7.
Thompson, C.F., Young, A.P., Dickson, M.E., 2019. Wave impacts on coastal cliffs: do bigger waves drive greater ground motion? Earth Surf. Process. Landforms 44, 2849–2860.
Van Der Werf, J., De Vet, P., Boersema, M., Bouma, T., Nolte, A., Schrijvershof, R., Soissons, L., Stronkhorst, J., Van Zanten, E., Ysebaert, T., 2019. An integral approach to design the Roggenplaat intertidal shoal nourishment. Ocean Coast Manag. 172, 30–40.
Veigas, M., López, M., Romillo, P., Carballo, R., Castro, A., Iglesias, G., 2015. A proposed wave farm on the Galician coast. Energy Convers. Manag. 99, 102–111.
Waldman, S., Baston, S., Nemalidinne, R., Chatzirodou, A., Venugopal, V., Side, J., 2017. Implementation of tidal turbines in mike 3 and delft3d models of pentland firth & orkney waters. Ocean Coast Manag. 147, 21–36.
Westoby, M.J., Lim, M., Hogg, M., Pound, M.J., Dunlop, L., Woodward, J., 2018. Cost-effective erosion monitoring of coastal cliffs. Coast. Eng. 138, 152–164.
Zelaya Wziatek, D., Terefenko, P., Kurylczyk, A., 2019. Multi-temporal cliff erosion analysis using airborne laser scanning surveys. Rem. Sens. 11, 2666.